PNAS RESEARCH ARTICLE | AGRICULTURAL SCIENCES

The CsHEC1-CsOVATE module contributes to fruit neck length variation via modulating auxin biosynthesis in cucumber

Zhongyi Wang[a], Zhaoyang Zhou[a], Liming Wang[a], Shuangshuang Yan[a], Zhihua Cheng[a], Xiaofeng Liu[a], Lijie Han[a], Guangxin Chen[a], Shaoyun Wang[a], Weiyuan Song[a], Jiacai Chen[a], Liu Liu[a], Xiaofei Song[b], Liying Yan[b], Jianyu Zhao[a,1], and Xiaolan Zhang[a,1]

Edited by Adrienne Roeder, Cornell University, Ithaca, NY; received June 16, 2022; accepted August 2, 2022 by Editorial Board Member Sean R. Cutler

Fruit neck is the proximal portion of the fruit with undesirable taste that has detrimental effects on fruit shape and commercial value in cucumber. Despite the dramatic variations in fruit neck length of cucumber germplasms, the genes and regulatory mechanisms underlying fruit neck elongation remain mysterious. In this study, we found that *Cucumis sativus HECATE1* (*CsHEC1*) was highly expressed in fruit neck. Knockout of *CsHEC1* resulted in shortened fruit neck and decreased auxin accumulation, whereas overexpression of *CsHEC1* displayed the opposite effects, suggesting that *CsHEC1* positively regulated fruit neck length by modulating local auxin level. Further analysis showed that CsHEC1 directly bound to the promoter of the auxin biosynthesis gene *YUCCA4* (*CsYUC4*) and activated its expression. Enhanced expression of *CsYUC4* resulted in elongated fruit neck and elevated auxin content. Moreover, knockout of *CsOVATE* resulted in longer fruit neck and higher auxin. Genetic and biochemical data showed that CsOVATE physically interacted with CsHEC1 to antagonize its function by attenuating the CsHEC1-mediated *CsYUC4* transcriptional activation. In cucumber germplasms, the expression of *CsHEC1* and *CsYUC4* positively correlated with fruit neck length, while that of *CsOVATE* showed a negative correlation. Together, our results revealed a CsHEC1-CsOVATE regulatory module that confers fruit neck length variation via *CsYUC4*-mediated auxin biosynthesis in cucumber.

cucumber | CsHEC1 | CsOVATE | fruit neck | auxin biosynthesis

Significance

Shape variations of plant edible organs are the result of adaptive evolution and domestication. Fruit neck is an undesirable trait that affects fruit shape and commercial value in cucumber. Despite fruit neck length (FNL) varying greatly among cucumber germplasms, the molecular mechanisms controlling FNL remain unknown. Here, we demonstrate that *HECATE1* (*CsHEC1*) positively regulates FNL by directly activating the auxin biosynthesis gene *CsYUC4*. CsOVATE, whose expression is negatively correlated with FNL, combats CsHEC1 to attenuate the CsHEC1-mediated *CsYUC4* transcriptional activation. Our work not only paves a way to shorten FNL by manipulating the CsHEC1-CsOVATE module to decrease local auxin levels during cucumber breeding but also provides significant insights into fruit shape regulation in pepo fruits.

The fruit is the prominent edible organ in horticultural crops that is essential for seed development and sexual reproduction. Fruit shape directly affects appearance quality and market value, and thus explosion in fruit shape variation is one of the hallmarks during crop domestication (1–3). So far, most fruit shape studies have been performed in tomato bearing the berry fruit, such as SUN, an IQ67-domain protein involved in Ca^{2+} signal transduction, acting as a positive regulator for elongated fruit shape, whereas the CLAVATA3/EMBRYO SURROUNDING REGION–related family member FASCIATED (FAS) and the WUSCHEL homeodomain protein LOCULE NUMBER (LC) function coordinately in fruit locule number controlling the flat shape (4–8). Cucumber is an important vegetable crop bearing the pepo fruit that is harvested immature at 8 to 18 d after anthesis, and consumed fresh or processed into pickles (9, 10). Morphologically, cucumber fruit consists of the fruit neck at the proximal end, connecting with the peduncle and the tasty fruit at the distal end (Fig. 1*A*). Fruit neck, also known as stalk or gynophore, usually has no spines/tubercules on the surface and no placenta inside (11–13). In cucumber germplasms, the fruit neck length (FNL) varies from 1 to 12 cm (Fig. 1*B*), which accounts for up to 35% of the total fruit length (2, 12). Due to the undesirable taste and the reduced diameter compared with that of the fruit, resembling a constricted neck, the fruit neck has detrimental effects on fruit shape and commercial value in cucumber (14).

Previous studies showed that FNL variation is controlled by additive genetic rather than environmental factors in cucumber (15, 16). In 2008, a major-effect quantitative trait locus (QTL) accounting for 18.5% in FNL was identified as located on a 21.4-cM region on chromosome 1 (17). Subsequently, four QTLs on chromosomes 3, 6, and 7 were detected by QTL mapping using 160 recombinant inbred lines (18). The first gene cloned for fruit neck elongation is *CsFnl7.1*, encoding a protein of the late embryogenesis abundant family, that may regulate fruit neck development by modulating cell expansion in cucumber (19). However, the regulatory mechanism underlying FNL variation remains largely unknown in cucumber.

Fruit neck is an important part of the apical–basal patterning of the fruit developed from the gynoecium, in which the arrangement of stigma, style, ovary, and fruit neck along the distal end to the proximal end constitutes the apical–basal axis of the gynoecium (Fig. 1 *A* and *C*) (11, 20, 21). Mutations in *HECATE* (*HEC*) genes, members of

Author contributions: Z.W., J.Z., and X.Z. designed research; Z.W., Z.Z., L.W., Z.C., X.L., and G.C. performed research; S.Y., L.H., S.W., W.S., J.C., and L.L. contributed new reagents/analytic tools; Z.W., Z.Z., L.W., X.S., and L.Y. analyzed data; and Z.W., J.Z., and X.Z. wrote the paper.

The authors declare no competing interest.

This article is a PNAS Direct Submission. A.R. is a guest editor invited by the Editorial Board.

[1]To whom correspondence may be addressed. Email: zhaojianyu@cau.edu.cn or zhxiaolan@cau.edu.cn.

This article contains supporting information online at http://www.pnas.org/lookup/suppl/doi:10.1073/pnas.2209717119/-/DCSupplemental.

Published September 19, 2022.

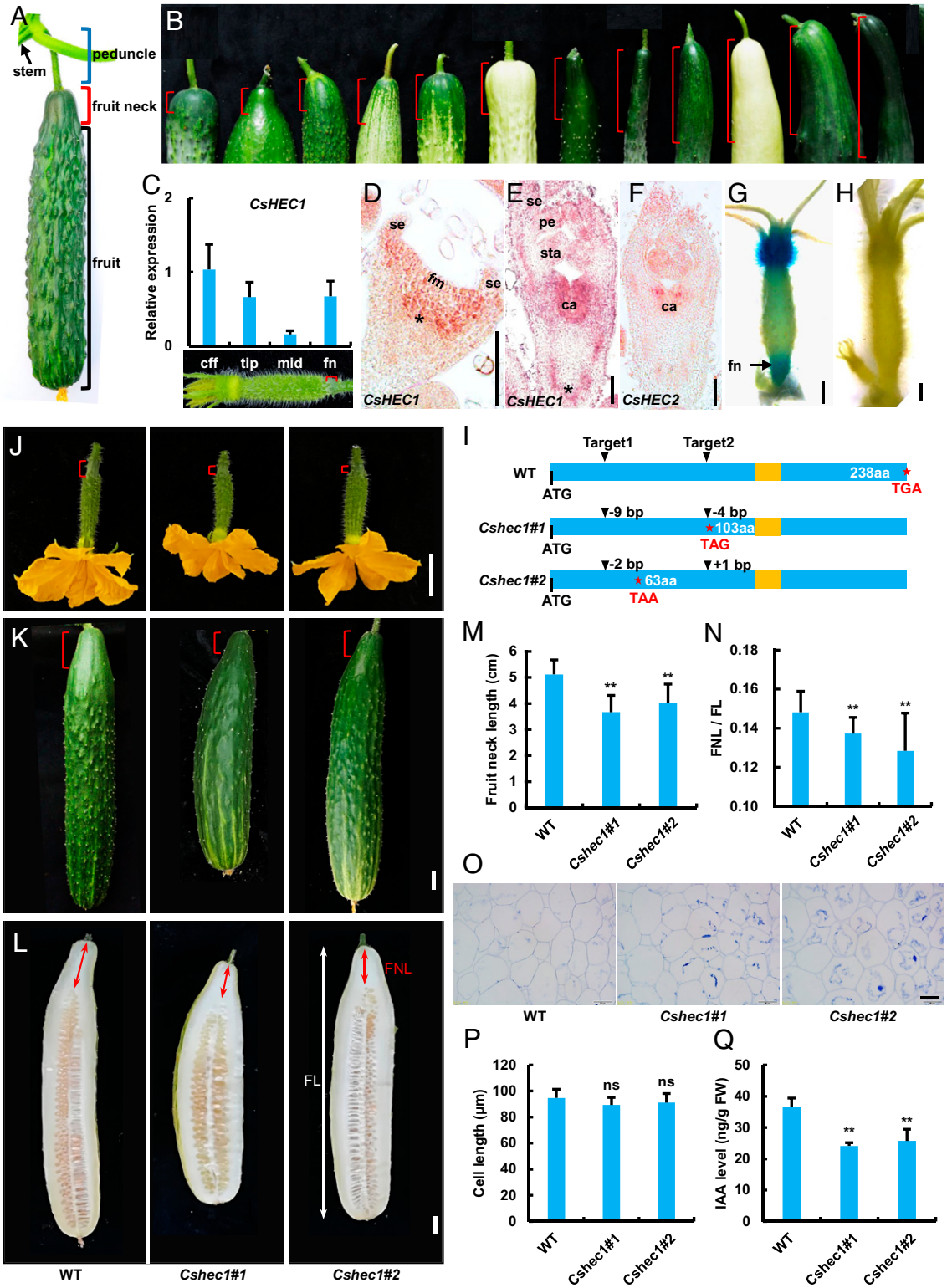

Fig. 1. Expression analysis of *CsHEC1* and phenotypic characterization of *CsHEC1* knockout lines in cucumber. (*A*) Structure of cucumber fruit at the commercial harvest stage. Blue bracket, peduncle; red bracket, fruit neck; black bracket, fruit. (*B*) Variations in FNL (red brackets) in different cucumber germplasms. (*C*) The expression pattern of *CsHEC1* in different parts of the ovary at 3 DBA. cff, corolla from the female flowers; fn, fruit neck; mid, middle. Values are means ± SD ($n = 3$). The red brackets indicate the fruit neck. (*D*–*F*) In situ hybridization analysis of *CsHEC1* (*D* and *E*) or *CsHEC2* (*F*) in cucumber. Longitudinal sections of developing flower primordium at stage 2 (*D*) and stage 6 (*E* and *F*). Asterisks indicate the developing fruit neck in cucumber. ca, carpel; fm, floral meristem; pe, petal; se, sepal; sta, stamen. (Scale bars, 100 μm.) (*G* and *H*) Tissue specificity of *CsHEC1* expression was examined using the *ProCsHEC1:GUS* reporter system. GUS signals of *CsHEC1* were highly enriched at the fruit neck and corolla of the female flower (*G*). Negative control showed no GUS signal (*H*). (Scale bars, 1 mm.) (*I*) Genotype identification of *CsHEC1* knockout plants indicated the *Cshec1#1* mutant with 9- and 4-bp deletions, and the *Cshec1#2* mutant with a 2-bp deletion and 1-bp insertion. The stars represent the termination codon position and the yellow boxes indicate the bHLH domain. (*J*–*L*) Morphology of WT, *Cshec1#1*, and *Cshec1#2* fruits at 0 DPP (*J*), 10 DPP (*K*), and 40 DPP (*L*). The red brackets indicate the fruit neck; the red and white double arrows represent the measured FNL and FL, respectively. (Scale bars, 2 cm.) (*M* and *N*) Quantification of FNL (*M*) and the ratio of FNL/FL (*N*) in WT and *Cshec1* mutants at 40 DPP. Values are means ± SD ($n = 10$). (*O* and *P*) Representative cell morphology (*O*) and cell-length quantification (*P*) of longitudinal sections of the fruit necks in WT and *Cshec1* fruits at 40 DPP. Values are means ± SD ($n = 9$). (Scale bar, 50 μm.) (*Q*) IAA content in the fruit necks of WT and *Cshec1* mutants. FW, fresh weight. Values are means ± SD ($n = 3$). Significance analysis compared with WT was performed with the two-tailed Student's *t* test (ns, no significant difference; $^{**}P < 0.01$).

the basic helix–loop–helix (bHLH) family, showed defects in transmitting tract and stigma formation leading to reduced fertility. Overexpression of *HEC1* or *HEC3* driven by the constitutive cauliflower mosaic virus 35S promoter occasionally produced gynoecia with defects in apical–basal polarity (22), resembling the loss of function in the auxin efflux carrier PIN-FORMED1 (PIN1) (23). Further study showed that HEC1 boosted auxin transport via directly stimulating the expression of *PIN1* and *PIN3* during gynoecium development in *Arabidopsis* (24).

OVATE family proteins (OFPs) were shown to regulate fruit shape and size in agricultural crops (25, 26). *OVATE* was the first gene identified in the OFPs as a repressor of fruit growth, and its loss-of-function mutation resulted in fruit transition from round- to pear-shaped with longitudinal elongation at the proximal end and obvious neck constriction in tomato (27, 28). SlOFP20, another member of the OFPs underlying the *suppressor of ovate* (*sov1*) locus, acted synergistically with OVATE resulting in a conspicuous pear-shaped tomato. OVATE and SlOFP20 interacted with several members of TONNEAU1 RECRUITMENT MOTIF (TRM) to regulate tomato fruit shape by fine-tuning cell-division patterns (26). In peach, transcriptional activation of *PpOFP1* caused by the 1.7-Mb chromosomal inversion event was responsible for flat-shaped fruit. PpOFP1 was the homologous protein of both AtOFP1 and SlOFP20, which may function as a transcriptional repressor of cell division or elongation, interacting with the elongation activator PpTRM17 (26, 29, 30). In addition, QTL mapping showed that several homologous genes to OFP and TRM members were encompassed in the chromosome regions specifying the shape change from round to elongated fruit in melon, cucumber, and potato; despite this, functional validation and regulatory mechanisms are mysterious (26, 31, 32).

In this study, we found that cucumber *CsHEC1* is highly expressed in the fruit neck region and plays a positive role in fruit neck elongation. Further analysis showed that CsHEC1 directly bound to the *CsYUC4* promoter and enhanced its expression, resulting in elevated auxin accumulation and increased FNL. Moreover, our data indicated that CsOVATE functions as a negative regulator for fruit neck elongation through physical interaction with CsHEC1 to attenuate the CsHEC1-mediated *CsYUC4* activation. A working model involved in the regulation of FNL variation by the CsHEC1-CsOVATE module through mediated auxin biosynthesis is proposed.

Results

Characterization of the CsHEC1 Transcription Factor in Cucumber. In the dehiscent silique of *Arabidopsis*, *HEC1/2/3* genes function redundantly during gynoecium development through controlling the formation of the transmitting tract and stigma (22, 24). In cucumber bearing fresh pepo fruit, our recent studies showed that CsHEC2 regulates fruit wart formation by stimulating cytokinin biosynthesis and irregular vasculature patterning (CsIVP); the CsHEC3 subfamily participates in both organ shape determination and downy mildew resistance via mediating vasculature development (33, 34). In this study, we characterized the function of CsHEC1 (Csa4G639900) during fruit development in cucumber. Phylogenetic analysis showed that Cucurbitaceae HEC1 and HEC2 belong to two different clades, and CsHEC1 is more closely related to HEC1 and HEC2 of *Arabidopsis* (*SI Appendix*, Fig. S1 and Table S1). Both CsHEC1 and CsHEC2 contain a conserved bHLH domain, but share only 41% amino acid identity across the full length of proteins (*SI Appendix*, Fig. S2) (35). Similar to the gene structure of *HEC1* and *HEC2* in *Arabidopsis*, the coding region of *CsHEC1* is 717 bp with a single exon (*SI Appendix*, Fig. S3*A*) (22). Subcellular localization assay indicated that CsHEC1 was localized in the nucleus (*SI Appendix*, Fig. S3*B*). Dual-luciferase reporter (DLR) assay showed that CsHEC1 exhibited higher luciferase activity compared with the control vector, similar to that of VP16 positive control (*SI Appendix*, Fig. S3*C*) (36), implying that CsHEC1 may act as a transcriptional activator located in the nucleus.

***CsHEC1* Is Highly Expressed in the Fruit Neck of Cucumber.** To explore the expression pattern of *CsHEC1*, three methods were performed in cucumber. qRT-PCR showed that *CsHEC1* transcripts were prominently enriched in ovaries 3 d before anthesis (DBA) (*SI Appendix*, Fig. S4*A*). Particularly, *CsHEC1* transcripts were highly accumulated in the corolla and fruit neck (Fig. 1*C*). RNA in situ hybridization analysis showed that *CsHEC1* signal was observed throughout the shoot apical meristem and floral meristem (*SI Appendix*, Fig. S4*B*). In floral buds at stages 1 to 4, strong signals were detected beneath the rib zone where the fruit neck will initiate (Fig. 1*D*, asterisk and *SI Appendix*, Fig. S4 *C–E*) (37). Upon stages 6 to 8, *CsHEC1* messenger RNAs were predominantly found in the developing carpels and fruit necks (Fig. 1*E* and *SI Appendix*, Fig. S4 *F* and *G*) and corolla (*SI Appendix*, Fig. S4 *H* and *I*). Importantly, *CsHEC2*, the paralogous gene of *CsHEC1*, was expressed in the carpel primordium, but not in the fruit neck (Fig. 1*F* and *SI Appendix*, Fig. S1). GUS (β-glucuronidase) reporter results further confirmed the high expression of *CsHEC1* in the fruit neck, corolla, and developing ovules (Fig. 1 *G* and *H* and *SI Appendix*, Fig. S4 *J* and *K*). These results indicated a potential role of *CsHEC1* in fruit neck development in cucumber.

***CsHEC1* Promotes Fruit Neck Elongation through Mediating Auxin Accumulation.** To explore the function of *CsHEC1* in cucumber, homozygous loss-of-function mutants were obtained using the CRISPR-Cas9 system in the inbred line XTMC, a North China–type cucumber with long fruits and medium FNL. Two mutant lines, *Cshec1#1* (with 9- and 4-bp deletions) and *Cshec1#2* (with a 2-bp deletion and 1-bp insertion) were identified for further characterizations (Fig. 1*I* and *SI Appendix*, Fig. S5*A*). No mutation was detected in the potential off-target sites of PCR sequencing products (*SI Appendix*, Table S2). Compared with wild-type (WT) plants, both mutants exhibited a shorter fruit neck from 0 d postpollination (DPP) to maturity in cucumber (Fig. 1 *J–L*). Quantification data analyses showed that the *Cshec1* mutants had 21 to 28% decreases in FNL (Fig. 1*M*). Similarly, the fruit length (FL) was decreased, and the ratio of FNL to FL (FNL/FL) was significantly reduced in *Cshec1* mutants (Fig. 1*N* and *SI Appendix*, Fig. S5*B*). Longitudinal sections of the fruit neck tissue from *Cshec1* mutants and WT plants showed no significant difference in cell length (Fig. 1 *O* and *P*), suggesting that *CsHEC1* may stimulate fruit neck elongation by mediating cell division. Previous studies indicated that auxin plays a unique role in regulating apical–basal fruit patterning in *Arabidopsis* and tomato (38–40). The auxin indole-3-acetic acid (IAA) level in fruit neck was greatly reduced in *Cshec1* mutants (Fig. 1*Q*), implying that *CsHEC1* may modulate local auxin accumulation during fruit neck development.

To further confirm *CsHEC1* function in cucumber fruit, a *CsHEC1* overexpression (OE) vector (*Pro35S:CsHEC1-Flag*) was constructed for genetic transformation. Five *CsHEC1*-OE transgenic lines were obtained and three representative lines (OE#2, OE#3, and OE#4) were selected for further analyses (Fig. 2).

The qRT-PCR result indicated that the expression levels of *CsHEC1* in the overexpression lines OE#2, OE#3, and OE#4 were 150-, 126-, and 95-fold higher than that of WT, respectively (Fig. 2*A*). Immunoblot assay demonstrated that the CsHEC1 protein had a high-level accumulation in all three OE transgenic lines (Fig. 2*B*). Compared with the WT, *CsHEC1*-OE fruits displayed remarkably elongated fruit neck from 0 DPP to maturity (Fig. 2 *C*–*E*). Quantification analyses showed that the *CsHEC1*-OE lines had 24 to 53% increases in FNL at maturity (Fig. 2*F*). No significant differences were detected in FL between WT and *CsHEC1*-OE lines (*SI Appendix*, Fig. S6*A*). Thus, the ratio of FNL/FL was significantly elevated in *CsHEC1*-OE lines (Fig. 2*G*). Longitudinal sections of the fruit neck at 40 DPP showed no consistent change in cell length (Fig. 2 *H* and *I*), suggesting that the main cause of fruit neck elongation may be increased cell numbers in *CsHEC1*-OE lines. Moreover, the IAA

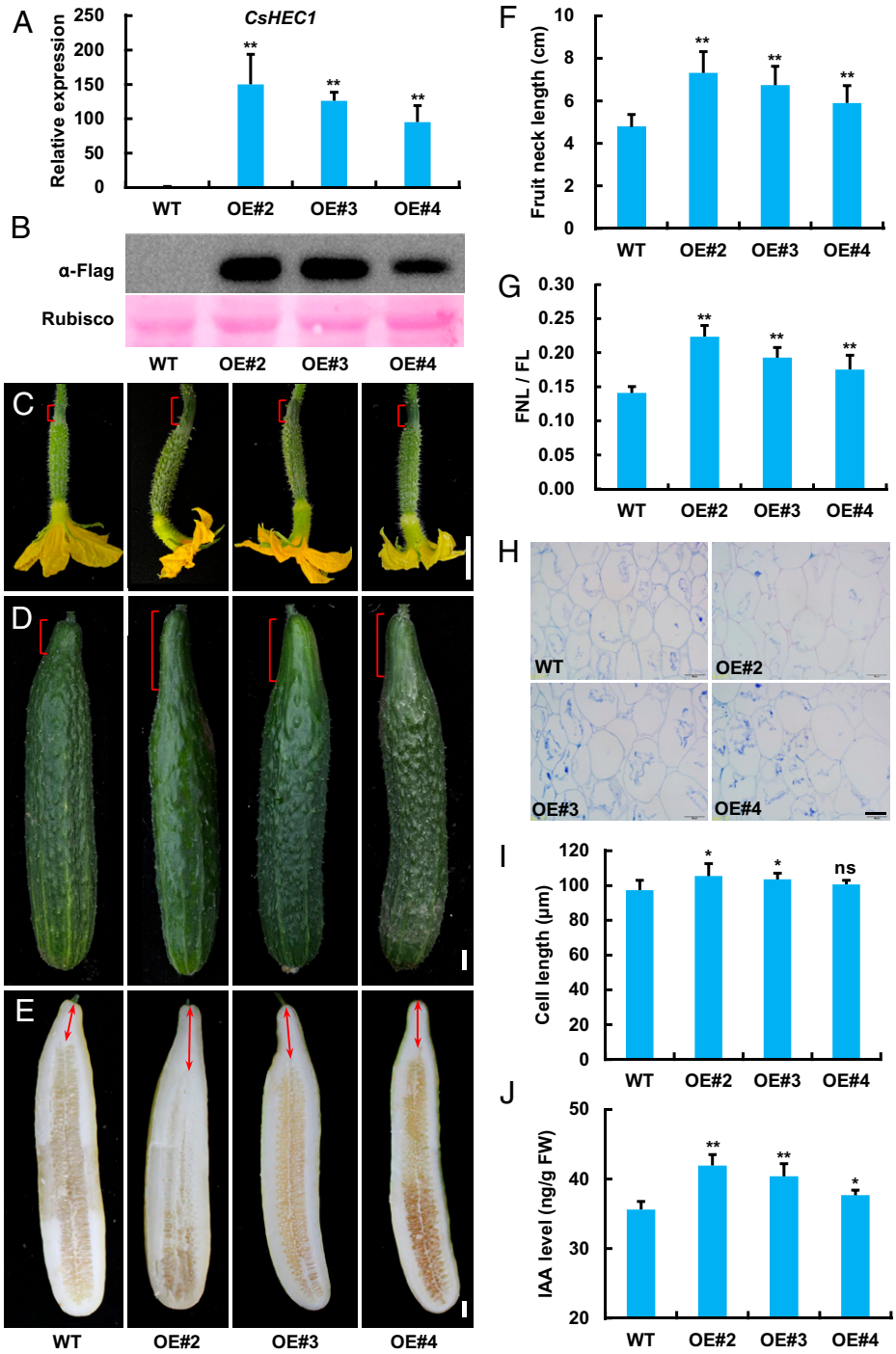

Fig. 2. Overexpression of *CsHEC1* results in elongated fruit neck in cucumber. (*A*) qRT-PCR analysis of *CsHEC1* expression in *CsHEC1*-OE lines. Values are means ± SD ($n = 3$). (*B*) Immunoblot analysis of CsHEC1 protein levels in *CsHEC1*-OE lines using anti-Flag antibody. Rubisco large subunit stained by Ponceau S served as a loading control. (*C*–*E*) Fruit phenotype of *CsHEC1*-OE transgenic plants at 0 DPP (*C*), 10 DPP (*D*), and 40 DPP (*E*). The brackets indicate the fruit neck, and the double arrows represent the measured FNL. (Scale bars, 2 cm.) (*F* and *G*) Quantification of FNL (*F*) and ratio of FNL/FL (*G*) in WT and *CsHEC1*-OE lines at 40 DPP. Values are means ± SD ($n = 6$). (*H* and *I*) Representative cell morphology (*H*) and cell-length quantification (*I*) of longitudinal sections of the fruit necks in WT and *CsHEC1*-OE fruits at 40 DPP. Values are means ± SD ($n = 9$). (Scale bar, 50 μm.) (*J*) IAA content in the fruit neck of WT and *CsHEC1*-OE plants. Values are means ± SD ($n = 3$). Significance analysis compared with WT was performed with the two-tailed Student's *t* test (ns, no significant difference; $^*P < 0.05$, $^{**}P < 0.01$).

level in fruit neck was greatly elevated in *CsHEC1*-OE lines (Fig. 2*J*). To explore whether the effect of *CsHEC1* on fruit neck elongation is ecotype-specific, overexpression of *CsHEC1* in a South China–type cucumber, GFC, bearing short fruits was performed. Similarly, our data showed that both FNL and auxin level were increased upon overexpression of *CsHEC1* in GFC (*SI Appendix*, Fig. S7), supporting that CsHEC1 positively regulated fruit neck elongation by promoting auxin accumulation in cucumber.

CsHEC1 Directly Activates the Auxin Biosynthesis Gene *CsYUC4* to Promote Fruit Neck Elongation. Members of the YUCCA (YUC) family mediate local auxin biosynthesis by catalyzing indole-3-pyruvic acid into IAA, the major naturally occurring auxin (41, 42). To explore whether CsHEC1 mediates auxin accumulation through auxin biosynthesis genes, the expression of 10 *CsYUC*s was examined in young stems and fruit necks in cucumber (43). Among them, the expression levels of *CsYUC10a* and *CsYUC11* were undetectable. Interestingly, only *CsYUC4* was highly expressed in the fruit neck compared with that in the stem (*SI Appendix*, Fig. S8). We further analyzed the expression level of *CsYUC4* in *CsHEC1* transgenic lines, and our data showed that transcripts of *CsYUC4* were significantly decreased in *Cshec1* mutants and greatly elevated in the *CsHEC1*-OE lines (Fig. 3 *A* and *B* and *SI Appendix*, Fig. S7*H*), suggesting that *CsHEC1* may promote auxin accumulation through enhancing *CsYUC4* expression.

The bHLH transcription factors were shown to directly bind to the variant "E box" (5′-CANNTG-3′) in the gene regulatory regions (44, 45). Two putative E-box elements (P1, -1199, 5′-CATTTG-3′; P2, -889, 5′-CAAATG-3′) in the *CsYUC4* promoter were identified (Fig. 3*C*). Yeast one-hybrid assay showed that CsHEC1 directly interacted with the P1 and P2 elements (Fig. 3*D*). Chromatin immunoprecipitation (ChIP)–PCR assays in transgenic cucumber plants showed that the P1 fragment was significantly enriched by CsHEC1-Flag, rather than by CsHEC2-Flag protein, after immunoprecipitation (Fig. 3*E*). A transactivation assay using the DLR system showed that the LUC/REN ratio was significantly increased upon coexpression of *ProCsYUC4:LUC* with *Pro35S:CsHEC1* but not with the empty vector *62-SK* or *Pro35S:CsHEC2* (Fig. 3*F*). Furthermore, electrophoretic mobility-shift assay further supported the direct binding of CsHEC1 to *CsYUC4* through the P1 element (Fig. 3*G*). These results suggest that CsHEC1 directly binds to the *CsYUC4* promoter to activate its expression.

To verify CsHEC1 stimulates fruit neck elongation through *CsYUC4*-mediated auxin biosynthesis, the *ProCsHEC1:CsYUC4* transgenic lines (YUC4#1 and YUC4#9) were generated. qRT-PCR analysis indicated the expression of *CsYUC4* was significantly increased in YUC4#9 and YUC4#1 lines compared with WT plants (Fig. 3*H*). As expected, elevated expression of *CsYUC4* resulted in a 17 to 25% increase in FNL and 12 to 24% elevation in the FNL/FL ratio (Fig. 3 *I*–*L*). The IAA level in fruit neck was also significantly increased in the *ProCsHEC1:CsYUC4* lines (Fig. 3*M*). Further, two *Csyuc4* mutants were generated using the CRISPR-Cas9 system, both of which resulted in significant reduction of FNL and decrease of fruit length, similar to the phenotype of *Cshec1* mutants (*SI Appendix*, Fig. S9). Taken together, these results suggested that CsHEC1 directly activated *CsYUC4* expression to enhance auxin accumulation and thus promoted fruit neck elongation in cucumber.

CsOVATE Negatively Regulates Fruit Neck Elongation in Cucumber. Overexpression of *CsHEC1* resulted in fruits with elongated fruit necks (Fig. 2 and *SI Appendix*, Fig. S7), reminiscent of the phenotype of the tomato *ovate* mutant (1, 27). To investigate whether CsOVATE (31), a homologous protein of tomato OVATE, regulates fruit neck development in cucumber, we first analyzed the expression pattern using an in situ hybridization assay. Similar to *CsHEC1*, the results showed that the *CsOVATE* signal was predominantly accumulated in the floral meristem, fruit neck, and carpel primordia (Fig. 4 *A*–*D*). Knockout mutant lines were obtained using the CRISPR-Cas9 system, and two homozygous *Csovate* mutants (*Csovate#1* with 1- and 7-bp deletions; *Csovate#2* with 3- and 1-bp deletions) resulting in premature stop codons were identified for further characterization (Fig. 4*E* and *SI Appendix*, Fig. S10*A* and Table S3). Loss of function of *CsOVATE* led to elongated fruit neck from 0 DPP to maturity (Fig. 4 *F*–*H*), similar to that in *CsHEC1*-OE lines. Quantification analysis showed that *Csovate* mutants had a 25 to 28% increase in FNL (Fig. 4*I*), and a larger ratio of FNL/FL than that in WT (Fig. 4*J* and *SI Appendix*, Fig. S10*B*). Longitudinal sections of the fruit neck tissue from *Csovate* fruits and WT plants showed no significant difference in cell length (Fig. 4 *K* and *L*), suggesting that *CsOVATE* negatively regulated fruit neck elongation by decreasing cell numbers in cucumber.

CsHEC1 Physically Interacts with CsOVATE at the Protein Level. Given the opposite roles of CsHEC1 and CsOVATE during fruit neck elongation (Figs. 1, 2, and 4), we next explored any interactions between CsHEC1 and CsOVATE. Expression analyses were performed in the counterpart's transgenic lines. The expression of *CsOVATE* was not altered in *Cshec1* mutants or *CsHEC1*-OE lines (*SI Appendix*, Figs. S5*C* and S6*B*). Likewise, the *CsHEC1* expression was unaffected in the *Csovate* mutants (*SI Appendix*, Fig. S10*C*), indicating no transcriptional regulation between CsHEC1 and CsOVATE in cucumber. Tomato OVATE was known to be localized in the cytoplasm of *Nicotiana benthamiana* leaf epidermal cells (26). However, CsOVATE-GFP (green fluorescent protein) had a localization signal both in the cytoplasm and in the nucleus, and CsOVATE colocalized with CsHEC1 in the nucleus (Fig. 5*A*). Yeast two-hybrid assay showed that CsHEC1 interacted with CsOVATE at the protein level (Fig. 5*B*). Pull-down experiment indicated that GST (glutathione S-transferase)-CsHEC1 was able to bind to His-CsOVATE (Fig. 5*C*). The firefly luciferase complementation imaging (LCI) assay in *N. benthamiana* showed that CsOVATE interacted with CsHEC1 but not with CsHEC2 (Fig. 5*D* and *SI Appendix*, Fig. S11). The specific interaction between CsOVATE and CsHEC1 was further verified by coimmunoprecipitation (Co-IP) analysis (Fig. 5*E*). Together, these results suggested that CsOVATE directly interacted with CsHEC1 at the protein level both in vitro and in vivo.

Genetic Interaction of CsOVATE with CsHEC1 in Cucumber. To determine the genetic relationships between *CsHEC1* and *CsOVATE*, we generated a double mutant by crossing *Csovate#1* with *Cshec1#1*. The FNLs of the double mutant *Csovate#1 Cshec1#1* were indistinguishable from those of *Cshec1#1* but markedly shorter than those of *Csovate#1* and WT (Fig. 6 *A*–*D*), suggesting that the function of CsOVATE is dependent on CsHEC1 during fruit neck elongation. Meanwhile, plants overexpressing *CsHEC1* (*Pro35S:CsHEC1-Flag*, OE#4) in the *Csovate#1* mutant were obtained and exhibited further elongated fruit neck and increased FNL/FL ratio at anthesis and maturity compared with *CsHEC1*-OE#4 (Fig. 6 and *SI Appendix*, Fig. S12). Immunoblot analysis showed that the corresponding CsHEC1 protein was overexpressed in the respective plants with

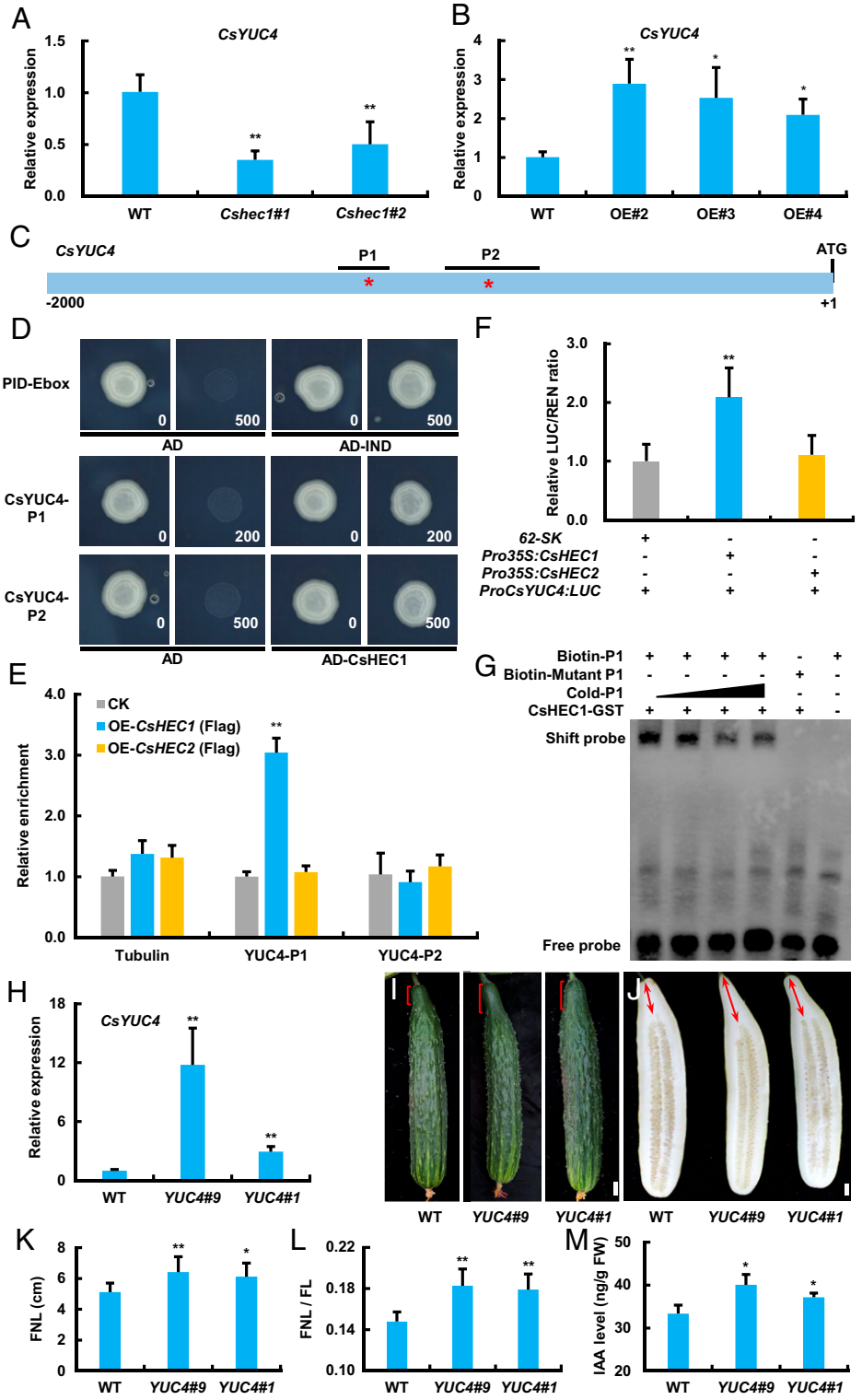

Fig. 3. CsHEC1 directly activates the expression of the auxin biosynthesis gene *CsYUC4* to promote fruit neck elongation. (*A* and *B*) Gene expression analysis of *CsYUC4* in *Cshec1* knockout mutants (*A*) and *CsHEC1*-OE lines (*B*). Values are means ± SD ($n = 3$). *$P < 0.05$, **$P < 0.01$ (Student's *t* test). (*C*) Schematic diagram of the putative E-box *cis*-elements in the *CsYUC4* promoter. Asterisks represent the locations of putative E-box *cis*-elements. Black lines represent the fragments used for ChIP-PCR in *E*. (*D*) Yeast one-hybrid analysis of the interaction between the CsHEC1 protein and the variant E box from the *CsYUC4* promoter. The interaction between IND-AD and the PID-E box was used as a positive control. (*E*) CsHEC1 binds to the *cis*-element P1 regions of the *CsYUC4* promoter in vivo by ChIP-PCR analysis. *Tubulin* was used as a negative control. (*F*) Firefly luciferase (LUC) and renilla reiformis luciferase (REN) activity measurement was performed in *N. benthamiana* leaves by coexpression of *Pro35S:CsHEC1* or *Pro35S:CsHEC2* and *ProCsYUC4:LUC*. The empty vector *pGreenII 62-SK* was used as the control. Values are means ± SD ($n = 3$ in *E*; $n = 5$ in *F*). **$P < 0.01$ (Student's *t* test). (*G*) Electrophoretic mobility-shift experiment showed that CsHEC1 binds to the P1 fragment of the *CsYUC4* promoter. (*H*) Expression analysis of *CsYUC4* in the *ProCsHEC1:CsYUC4* transgenic lines. (*I* and *J*) Fruit morphology at 10 DPP (*I*) and 40 DPP (*J*) in WT and *ProCsHEC1:CsYUC4* plants. The brackets indicate the fruit neck; the double arrows represent the measured FNL. (Scale bars, 2 cm.) (*K* and *L*) Quantification of FNL (*K*) and ratio of FNL/FL (*L*) in WT and *ProCsHEC1:CsYUC4* lines at 40 DPP. (*M*) IAA content in the fruit neck of WT and *ProCsHEC1:CsYUC4* plants. Values are means ± SD ($n = 3$ in *H* and *M*; $n = 7$ in *K* and *L*). Significance analysis compared with WT was performed with the two-tailed Student's *t* test (*$P < 0.05$, **$P < 0.01$).

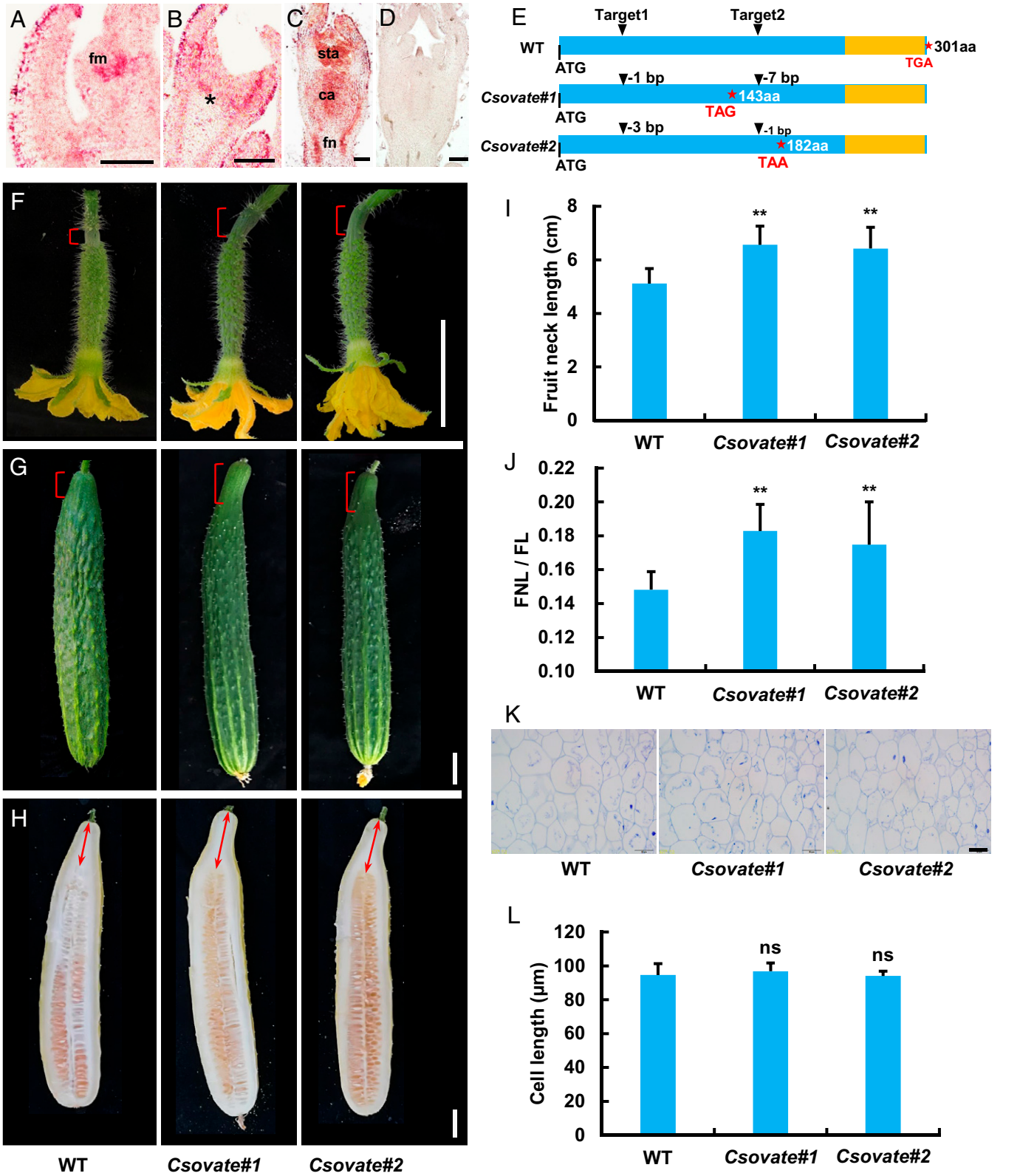

Fig. 4. *CsOVATE* negatively regulates fruit neck elongation in cucumber. (*A*–*D*) In situ hybridization analysis of *CsOVATE* expression in cucumber. Longitudinal sections showing floral meristem (*A*) and developing flower primordia at stage 2 (*B*) and stage 6 (*C*). The asterisk indicates the developing fruit neck in cucumber. The negative control hybridized with the sense *CsOVATE* probe (*D*). (Scale bars, 100 μm.) (*E*) CRISPR-Cas9–induced homozygous mutations in *CsOVATE* producing knockout alleles due to early appearance of stop codons. The stars represent the termination codon position and the yellow boxes indicate the OVATE domain. (*F*–*H*) Fruit morphology of WT and *Csovate* mutants at 0 DPP (*F*), 10 DPP (*G*), and 40 DPP (*H*). The brackets indicate the fruit neck and the double arrows represent the measured FNL. (Scale bars, 2 cm.) (*I* and *J*) Quantification of FNL (*I*) and ratio of FNL/FL (*J*) in WT and *Csovate* mutants at 40 DPP. Values are means ± SD (n = 9 to 14). (*K* and *L*) Representative cell morphology (*K*) and cell-length quantification (*L*) in the longitudinal sections of fruit necks in WT and *Csovate* fruits at 40 DPP. Values are means ± SD (n = 9). (Scale bar, 50 μm.) Significance analysis compared with WT was performed with the two-tailed Student's t test (ns, no significant difference; $^{**}P < 0.01$).

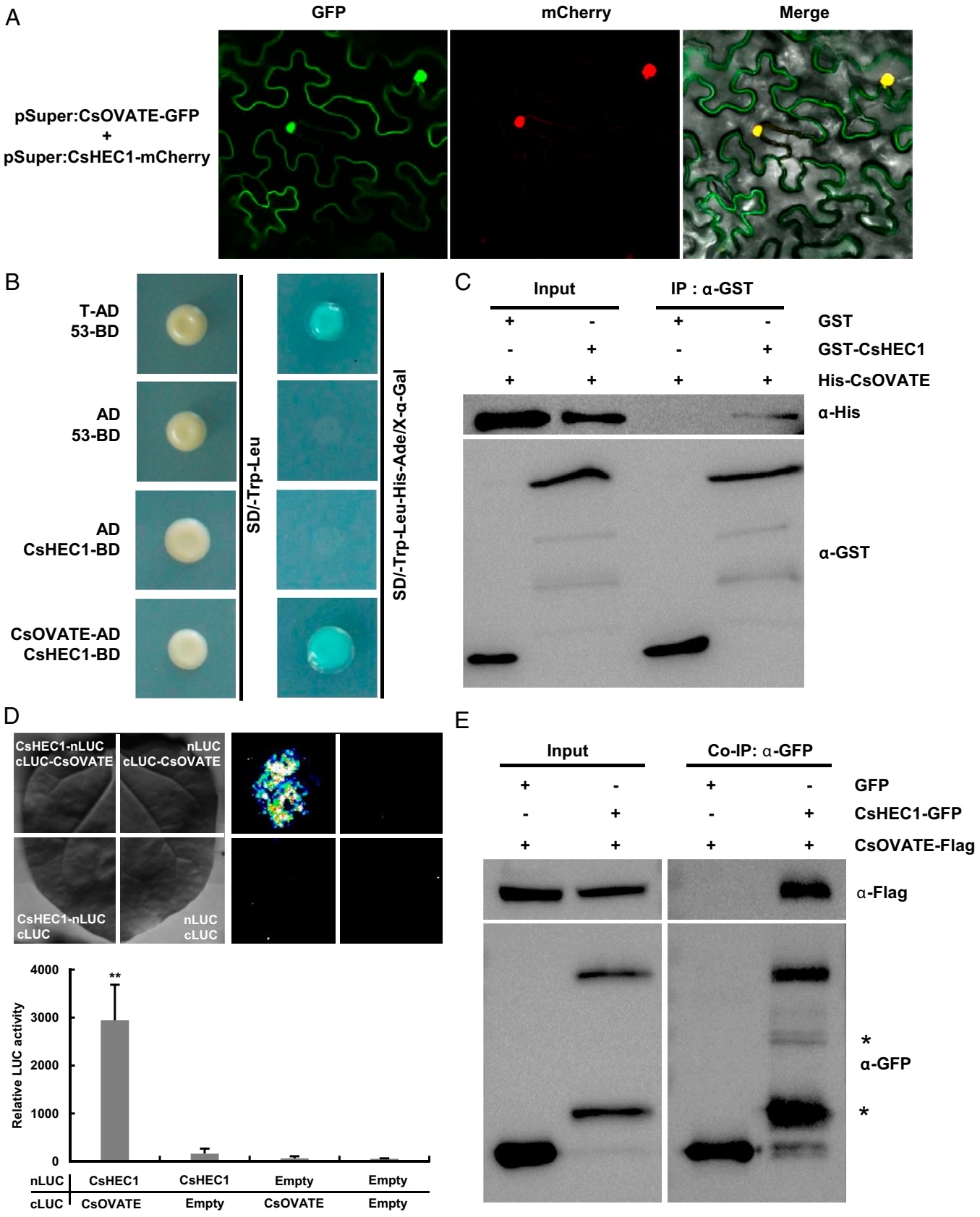

Fig. 5. CsHEC1 directly interacts with CsOVATE at the protein level. (*A*) CsOVATE colocalization with the CsHEC1 protein in *N. benthamiana* leaves. The yellow signal in the merged field represents the colocalization signal in the nucleus. (*B*) Interaction of CsHEC1 and CsOVATE in the yeast two-hybrid system. The combination of T-AD and 53-BD was used as a positive control. (*C*) CsHEC1 interacts with CsOVATE in vitro tested by a GST pull-down assay. The combination of GST and His-CsOVATE was used as a control. (*D*) Firefly luciferase complementation imaging analysis. CsHEC1-nLUC and cLUC-CsOVATE were transiently coexpressed in *N. benthamiana*, and the remaining combinations were used as controls. Representative pictures (*Top*) and the relative luciferase activity value are shown (*Bottom*). Values are means ± SD ($n = 6$). Two-tailed Student's *t* test (**$P < 0.01$). (*E*) Co-IP assay showing that CsHEC1 interacted with CsOVATE in vivo. The total and precipitated proteins were detected by immunoblotting using anti-GFP antibody or anti-Flag antibody. The asterisks indicate nonspecific bands.

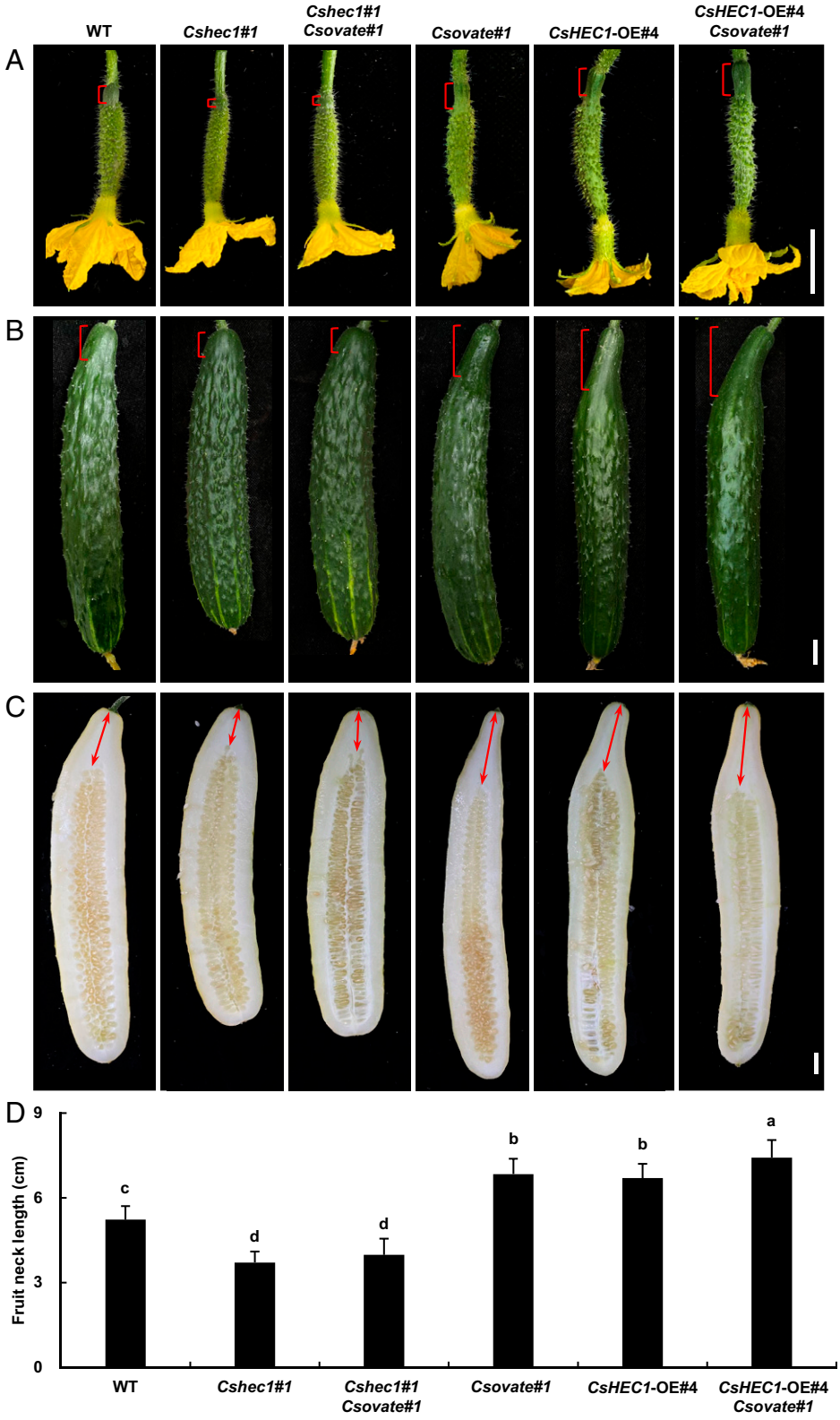

Fig. 6. Genetic interaction of CsOVATE and CsHEC1 during fruit neck elongation in cucumber. (*A*–*C*) Fruit morphology of WT, *Cshec1#1*, *Cshec1#1 Csovate#1*, *Csovate#1*, *CsHEC1*-OE#4, and *CsHEC1*-OE#4/*Csovate#1* at 0 DPP (*A*), 10 DPP (*B*), and 40 DPP (*C*). The brackets indicate the fruit neck and the double arrows represent the measured FNL. (Scale bars, 2 cm.) (*D*) Quantification of FNLs in the indicated lines at maturity. Values are means ± SD ($n = 7$). The different lowercase letters indicate significant differences ($P < 0.05$) by one-way ANOVA analysis with Duncan's test.

similar expression levels (*SI Appendix*, Fig. S13). Together, these data suggested that CsOVATE genetically interacted with CsHEC1 to inhibit CsHEC1 function in regulating fruit neck elongation in cucumber.

CsOVATE Attenuates CsHEC1-Mediated *CsYUC4* Activation and Auxin Accumulation. To further dissect the causal relationship between CsHEC1 and CsOVATE in the natural cucumber population, the expression of *CsHEC1*, *CsYUC4*, and *CsOVATE*

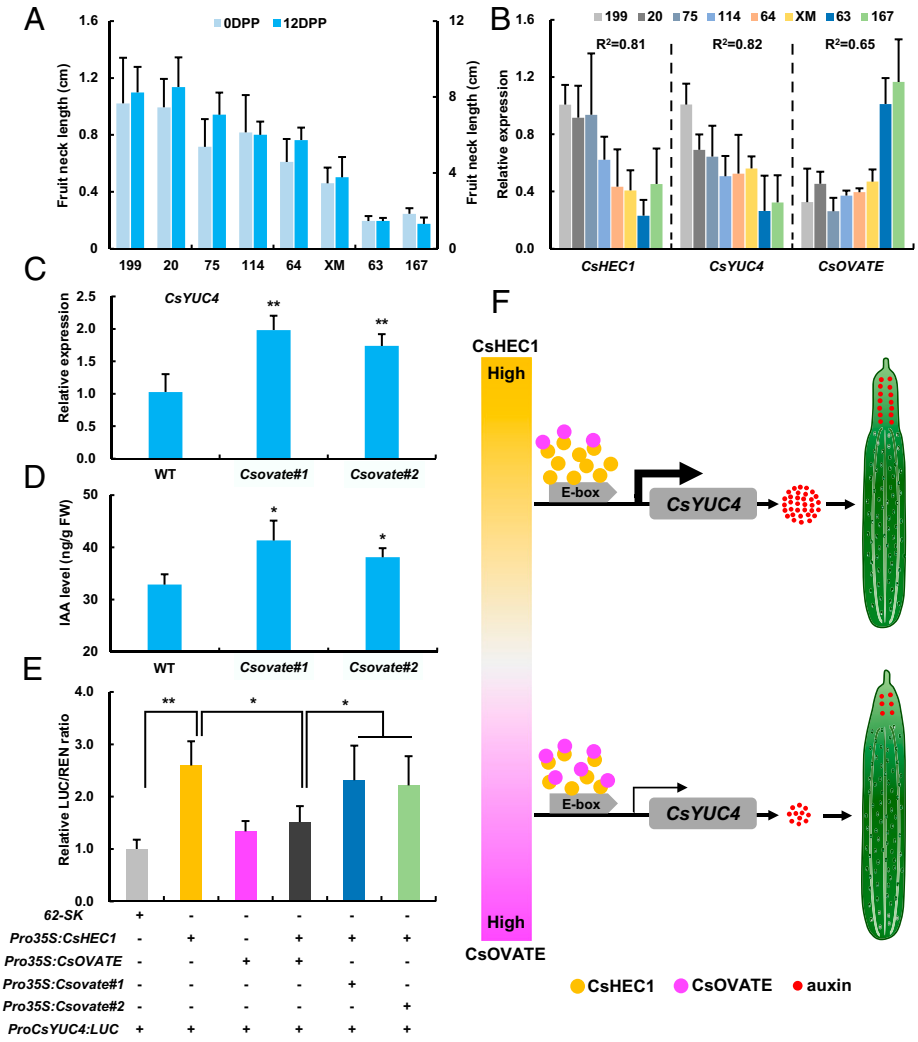

Fig. 7. CsOVATE antagonizes CsHEC1-mediated *CsYUC4* activation during fruit neck elongation in cucumber. (*A*) Cucumber inbred lines with different FNL at 0 and 10 DPP. (*B*) Expression analysis of *CsHEC1*, *CsYUC4*, and *CsOVATE* in different cucumber inbred lines. (*C*) Expression analysis of *CsYUC4* in WT and *Csovate* mutants. (*D*) IAA content in the fruit necks of WT and *Csovate* mutants. Values are means ± SD ($n = 3$ in *C* and *D*). (*E*) Firefly luciferase and renilla reiformis luciferase activity assay in *N. benthamiana* leaves by coexpression of *Pro35S:CsHEC1* and/or *Pro35S:CsOVATE* or *Pro35S:Csovate#1* or *Pro35S:Csovate#2* with *ProCsYUC4:LUC*. Values are means ± SD ($n = 5$). Significance analysis was calculated by Student's *t* test (*$P < 0.05$, **$P < 0.01$). (*F*) The working model of CsHEC1 and CsOVATE regulating fruit neck elongation in cucumber. CsHEC1 promotes fruit neck elongation in cucumber by directly activating the expression of *CsYUC4* and thus increasing auxin accumulation in the fruit neck. CsOVATE functions as a negative regulator for fruit neck elongation via interaction with CsHEC1 to attenuate the CsHEC1-mediated *CsYUC4* activation, thus reducing auxin biosynthesis in the fruit neck.

was analyzed in eight cucumber inbred lines with different FNLs. Our data showed that the expression of *CsHEC1* and *CsYUC4* was positively correlated with FNL, with the correlation coefficient R^2 0.81 for *CsHEC1* and 0.82 for *CsYUC4*, whereas the expression of *CsOVATE* displayed a negative correlation (Fig. 7 *A* and *B*). Both *CsYUC4* expression and auxin level were significantly increased in the fruit neck of *Csovate* knockout lines (Fig. 7 *C* and *D*), suggesting that *CsOVATE* may inhibit fruit neck elongation via decreasing the *CsYUC4*-mediated auxin biosynthesis. To further explore the relationship between CsOVATE and *CsYUC4*, a DLR assay was performed. Unlike the direct transcriptional activation of *CsYUC4* by CsHEC1, the *CsYUC4* expression was unaffected upon coexpression of CsOVATE. However, *CsYUC4* transcription was significantly decreased upon coexpression of both CsOVATE and CsHEC1, while mutations of CsOVATE were unable to execute the attenuating effects (Fig. 7*E*), suggesting that CsOVATE antagonizes with CsHEC1 to modulate *CsYUC4* transcriptional activation and auxin biosynthesis during fruit neck development in cucumber.

Discussion

Unique Role of *CsHEC1* during Fruit Neck Elongation in Cucumber. The *HEC* genes encoding bHLH transcription factors play important roles in gynoecium development and shoot apical meristem maintenance (22, 24, 46). Here, we found that *CsHEC1* was highly expressed in the fruit neck and promoted fruit neck elongation in cucumber (Figs. 1 and 2 and *SI Appendix*, Figs. S5–S7). Gene function is usually closely related to the gene expression pattern, modulated by upstream regulatory proteins and *cis*-regulatory elements (5, 6, 47–50). Variations in regulatory regions or expression domains have been found to be the main causes for the remarkable diversity in organ morphology during natural evolution and the domestication process of crops (5, 47, 49). In *Arabidopsis*, *HEC1/2/3* are expressed in the female reproductive tissues, including stigma, style, septum, and transmitting tract. Accordingly, *hec* mutants display defects in the development of the stigma, transmitting tract, and septum, resulting in reduced fertility (22). In cucumber, *CsHEC1* was highly expressed in the fruit neck and its

mutation led to a shortened fruit neck, while *CsHEC2* was expressed in the spine and tubercule and functions in wart density control (34), suggesting the functional diversification of HECs in the fleshy pepo fruit. Interestingly, *CsHEC1* was highly expressed in the developing carpels as well while no aberrant carpel phenotype was observed in the *Cshec1* mutant, which may be due to overlapping expression of the paralogous genes *CsHEC2* and *CsHEC3* in carpel primordium and thus the exertion of redundant functions during carpel development in cucumber (33) (Fig. 1 *E* and *F* and *SI Appendix*, Fig. S1).

Gene duplication event is another important cause for neofunctionalization in homologous genes (51). Differentiation of the HEC1/2 clade and HEC3/INDEHISCENT (IND) clade resulted from an early duplication event in angiosperms (33, 52). Within Solanaceae, the HEC1 clade and HEC2 clade have undergone further duplications producing SlHEC1 and SlHEC1-1, and SlHEC2 and SlHEC2-1 (*SI Appendix*, Fig. S1), which generally are not expressed in the gynoecium of dry dehiscent or fleshy fruits in this family (52). Unlike the apparent functional redundancy of *HEC1/2/3* in *Arabidopsis*, *CsHEC1/2* contribute to fruit development, while *CsHEC3* regulates organ morphology and downy mildew resistance in cucumber (22, 33, 34). Thus, functional variations of HECs can be explained by their different expression patterns or duplication events in plant species with different fruit types.

CsHEC1 Regulates Auxin Biosynthesis to Promote Fruit Neck Elongation. The phytohormone auxin plays a crucial role in multiple developmental processes including organ morphogenesis and plant architecture determination (38, 49, 53, 54). The IND in *Capsella rubella* exerts its function on the heart-shaped fruit by directly stimulating the expression of auxin biosynthesis genes *TRYPTOPHAN AMINOTRANSFERASE OF ARABIDOPSIS 1* (*CrTAA1*) and *CrYUC9* to facilitate auxin maxima in the fruit shoulder (49). Auxin transporters PIN1/7 and PIN3 have been shown to mediate fruit elongation and shoot branching in cucumber, respectively (3, 54). In *Arabidopsis*, HEC1 functions in stigma formation and carpel fusion by directly activating the expression of *PIN1/3* (24). Although sporadic results of gene expression or genetic data suggest the possibility of regulation between HECs and YUCs (24), the direct relationship between HECs and YUCs has not been established.

Here, we showed that CsHEC1 stimulates auxin accumulation in the fruit neck in cucumber (Figs. 1*Q* and 2*J* and *SI Appendix*, Fig. S7*I*). Among the *CsYUC* family, *CsYUC4* is the only one displaying enriched expression in the fruit neck (*SI Appendix*, Fig. S8). Our data showed that CsHEC1 directly bound to the promoter of *CsYUC4* to activate its expression. Enhanced expression of *CsYUC4* driven by the *CsHEC1* promoter resulted in an elongated fruit neck and increased auxin level in cucumber (Fig. 3). *Csyuc4* mutants displayed shortened fruit neck and reduced fruit length (*SI Appendix*, Fig. S9), similar to that of *Cshec1* mutants. In cucumber inbred lines with different FNLs, the expression of *CsHEC1* and *CsYUC4* displayed positive correlation with FNL (Fig. 7 *A* and *B*). These data suggested that CsHEC1 functions as an activator for FNL through direct regulation of *CsYUC4*-mediated auxin biosynthesis in cucumber (Fig. 7*F*).

CsOVATE Combats CsHEC1 during Fruit Neck Elongation in Cucumber. Similar to the tomato fruit changing from round- to pear-shaped upon mutation in the *OVATE* gene (1, 27), *Csovate* mutants displayed increased FNL in cucumber (Fig. 4), suggesting that the function of OVATE appeared to be conserved in different species. The pear-shaped fruit caused by *OVATE* mutation in tomato was primarily due to an increase of the proximal cell numbers, resembling the effect of auxin application on fruit shape (40). In *Csovate* mutants, the longitudinal cell length was comparable to WT (Fig. 4 *K* and *L*), implying that the elongated fruit neck was due to an increase in cell numbers. The expression of *CsYUC4* and IAA level was greatly increased in the *Csovate* knockout lines (Fig. 7 *C* and *D*). However, no direct regulation of *CsYUC4* expression was detected by CsOVATE (Fig. 7*E*). Instead, CsOVATE directly interacts with CsHEC1 at the protein level (Fig. 5), and such interaction inhibits the *CsHEC1*-mediated transcriptional activation of *CsYUC4* (Fig. 7*E*). Genetic analysis showed that plants overexpressing *CsHEC1* in the *Csovate#1* mutant background exhibited further elongation of fruit neck than that of *CsHEC1*-OE#4 alone, while the FNL of the double mutant *Csovate Cshec1* resembles that of *Cshec1* (Fig. 6). In the natural cucumber population, *CsOVATE* expression is negatively correlated with FNL and *CsYUC4* transcription (Fig. 7 *A* and *B*). These data indicated that CsOVATE functions as a negative regulator for fruit neck elongation through direct interaction with CsHEC1 to attenuate the *CsYUC4*-mediated auxin biosynthesis. Thus, CsHEC1 and CsOVATE form a regulatory module to regulate local auxin content during controlling fruit neck elongation in cucumber (Fig. 7*F*). These findings provide a strategy to minimize the undesirable FNL by adjusting the levels of *CsHEC1* and/or *CsOVATE* transcription to decrease auxin accumulation in fruit neck during cucumber breeding.

Further studies are needed to dissect the promoter differences and the underlying regulatory mechanism of *CsHEC1* and *CsOVATE* expression in cucumber germplasms with various FNLs. Notably, similar to multiple regulators underlying fruit length variation in cucumber (3, 9, 55, 56), loss-of-function *Cshec1* mutants showed only 21 to 28% decreases in FNL (Fig. 1*M*), suggesting that additional genes such as *CsFnl7.1* (19) and other unidentified players may be involved in fruit neck development in cucumber. It would be of significant importance to dissect the gene network controlling fruit neck variation so as to accelerate genetic improvement of fruit shape in cucumber.

Materials and Methods

The details and procedures of plant materials and growth conditions, phenotypic characterization, phylogenetic analysis, generation of transgenic cucumber plants, subcellular localization, RNA extraction and expression analysis (qRT-PCR, in situ hybridization, and GUS staining), DNA–protein interaction assays (yeast one-hybrid, DLR, and ChIP-PCR), protein–protein interaction assays (yeast two-hybrid, LCI, pull-down, and Co-IP), and quantification of endogenous auxin and histology observation are provided in *SI Appendix*, *Materials and Methods*. Accession numbers used in this study are listed in *SI Appendix*, Table S1. Primers used in this study are provided in *SI Appendix*, Table S4.

Data, Materials, and Software Availability. All study data are included in the article and/or *SI Appendix*.

ACKNOWLEDGMENTS. We thank Prof. Sanwen Huang (Agricultural Genomics Institute at Shenzhen, Chinese Academy of Agricultural Sciences) for giving CRISPR-Cas9 vectors, and Dr. Li Yang for guidance in the cucumber transformation experiment. We are grateful to Prof. Xuexian Li (China Agricultural University) for critical comments. This work is supported by grants from the National Natural Science Foundation of China (32025033, 31930097, and 32102387), National Key Research and Development Program (2018YFD1000800), Construction of Beijing Science and Technology Innovation and Service Capacity in Top Subjects (CEFFPXM2019_014207_000032), and 111 Project (B17043).

Author affiliations: [a]State Key Laboratory of Agrobiotechnology, Joint International Research Laboratory of Crop Molecular Breeding, Beijing Key Laboratory of Growth and Developmental Regulation for Protected Vegetable Crops, Department of Vegetable Sciences, China Agricultural University, Beijing 100193, China; and [b]College of Horticulture Science and Technology, Hebei Normal University of Science and Technology, Qinhuangdao 066004, China

1. G. R. Rodríguez *et al.*, Distribution of *SUN*, *OVATE*, *LC*, and *FAS* in the tomato germplasm and the relationship to fruit shape diversity. *Plant Physiol.* **156**, 275–285 (2011).
2. J. Qi *et al.*, A genomic variation map provides insights into the genetic basis of cucumber domestication and diversity. *Nat. Genet.* **45**, 1510–1515 (2013).
3. J. Zhao *et al.*, A functional allele of *CsFUL1* regulates fruit length through repressing *CsSUP* and inhibiting auxin transport in cucumber. *Plant Cell* **31**, 1289–1307 (2019).
4. H. Xiao, N. Jiang, E. Schaffner, E. J. Stockinger, E. van der Knaap, A retrotransposon-mediated gene duplication underlies morphological variation of tomato fruit. *Science* **319**, 1527–1530 (2008).
5. B. Cong, L. S. Barrero, S. D. Tanksley, Regulatory change in YABBY-like transcription factor led to evolution of extreme fruit size during tomato domestication. *Nat. Genet.* **40**, 800–804 (2008).
6. S. Muños *et al.*, Increase in tomato locule number is controlled by two single-nucleotide polymorphisms located near *WUSCHEL*. *Plant Physiol.* **156**, 2244–2254 (2011).
7. Y. H. Chu, J. C. Jang, Z. Huang, E. van der Knaap, Tomato locule number and fruit size controlled by natural alleles of *lc* and *fas*. *Plant Direct* **3**, e00142 (2019).
8. C. Xu *et al.*, A cascade of arabinosyltransferases controls shoot meristem size in tomato. *Nat. Genet.* **47**, 784–792 (2015).
9. Y. Weng *et al.*, QTL mapping in multiple populations and development stages reveals dynamic quantitative trait loci for fruit size in cucumbers of different market classes. *Theor. Appl. Genet.* **128**, 1747–1763 (2015).
10. G. Che, X. Zhang, Molecular basis of cucumber fruit domestication. *Curr. Opin. Plant Biol.* **47**, 38–46 (2019).
11. A. H. Roeder, M. F. Yanofsky, Fruit development in *Arabidopsis*. *Arabidopsis Book* **4**, e0075 (2006).
12. J. Zhao *et al.*, Phloem transcriptome signatures underpin the physiological differentiation of the pedicel, stalk and fruit of cucumber (*Cucumis sativus* L.). *Plant Cell Physiol.* **57**, 19–34 (2016).
13. X. Sui *et al.*, Transcriptomic and functional analysis of cucumber (*Cucumis sativus* L.) fruit phloem during early development. *Plant J.* **96**, 982–996 (2018).
14. N. E. Fanourakis, E. E. Tzifaki, Correlated inheritance of fruit neck with fruit length and linkage relations with 10 other characteristics of cucumber. *Euphytica* **65**, 71–77 (1992).
15. X. Gu, X. Fang, X. Han, Preliminary study of fruit neck length inheritance in cucumber [in Chinese]. *China Vegetables* **2**, 33–34 (1994).
16. D. Ma, S. Lu, W. Shen, Z. Huo, S. Li, Combining ability analysis of cucumber quality characteristics [in Chinese]. *Acta Agriculturae Boreali–Sinica* **9**, 65–68 (1994).
17. G. Wang, Z. Qin, X. Zhou, Z. Zhao, Mapping quantitative trait loci influencing cucumber carpopodium length using simple sequence repeat markers [in Chinese]. *Acta Horticulturae Sinica* **35**, 543–546 (2008).
18. M. Wang *et al.*, Quantitative trait loci associated with fruit length and stalk length in cucumber using RIL population [in Chinese]. *Acta Bot. Boreali–Occidential Sinica* **34**, 1764–1770 (2014).
19. X. Xu *et al.*, The major-effect quantitative trait locus *Fnl7.1* encodes a late embryogenesis abundant protein associated with fruit neck length in cucumber. *Plant Biotechnol. J.* **18**, 1598–1609 (2020).
20. R. A. Sessions, P. C. Zambryski, *Arabidopsis* gynoecium structure in the wild and in *ettin* mutants. *Development* **121**, 1519–1532 (1995).
21. N. Marsch-Martínez, S. de Folter, Hormonal control of the development of the gynoecium. *Curr. Opin. Plant Biol.* **29**, 104–114 (2016).
22. K. Gremski, G. Ditta, M. F. Yanofsky, The *HECATE* genes regulate female reproductive tract development in *Arabidopsis thaliana*. *Development* **134**, 3593–3601 (2007).
23. K. Okada, J. Ueda, M. K. Komaki, C. J. Bell, Y. Shimura, Requirement of the auxin polar transport system in early stages of *Arabidopsis* floral bud formation. *Plant Cell* **3**, 677–684 (1991).
24. C. Schuster, C. Gaillochet, J. U. Lohmann, *Arabidopsis HECATE* genes function in phytohormone control during gynoecium development. *Development* **142**, 3343–3350 (2015).
25. A. Snouffer, C. Kraus, E. van der Knaap, The shape of things to come: Ovate family proteins regulate plant organ shape. *Curr. Opin. Plant Biol.* **53**, 98–105 (2020).
26. S. Wu *et al.*, A common genetic mechanism underlies morphological diversity in fruits and other plant organs. *Nat. Commun.* **9**, 4734 (2018).
27. J. Liu, J. Van Eck, B. Cong, S. D. Tanksley, A new class of regulatory genes underlying the cause of pear-shaped tomato fruit. *Proc. Natl. Acad. Sci. U.S.A.* **99**, 13302–13306 (2002).
28. D. Liu *et al.*, Phylogenetic analyses provide the first insights into the evolution of OVATE family proteins in land plants. *Ann. Bot.* **113**, 1219–1233 (2014).
29. S. Wang, Y. Chang, J. Guo, J. G. Chen, *Arabidopsis* Ovate family protein 1 is a transcriptional repressor that suppresses cell elongation. *Plant J.* **50**, 858–872 (2007).
30. H. Zhou *et al.*, A 1.7-Mb chromosomal inversion downstream of a *PpOFP1* gene is responsible for flat fruit shape in peach. *Plant Biotechnol. J.* **19**, 192–205 (2021).
31. Y. Pan *et al.*, Genetic architecture of fruit size and shape variation in cucurbits: A comparative perspective. *Theor. Appl. Genet.* **133**, 1–21 (2020).
32. J. Ma *et al.*, CmFSI8/CmOFP13 encoding an OVATE family protein controls fruit shape in melon. *J. Exp. Bot.* **73**, 1370–1384 (2022).
33. S. Yan *et al.*, CsIVP functions in vasculature development and downy mildew resistance in cucumber. *PLoS Biol.* **18**, e3000671 (2020).
34. Z. Wang *et al.*, HECATE2 acts with GLABROUS3 and Tu to boost cytokinin biosynthesis and regulate cucumber fruit wart formation. *Plant Physiol.* **187**, 1619–1635 (2021).
35. M. A. Heim *et al.*, The basic helix-loop-helix transcription factor family in plants: A genome-wide study of protein structure and functional diversity. *Mol. Biol. Evol.* **20**, 735–747 (2003).
36. Y. Xu *et al.*, A zinc finger protein BBX19 interacts with ABF3 to affect drought tolerance negatively in chrysanthemum. *Plant J.* **103**, 1783–1795 (2020).
37. S. L. Bai *et al.*, Developmental analyses reveal early arrests of the spore-bearing parts of reproductive organs in unisexual flowers of cucumber (*Cucumis sativus* L.). *Planta* **220**, 230–240 (2004).
38. J. L. Nemhauser, L. J. Feldman, P. C. Zambryski, Auxin and *ETTIN* in *Arabidopsis* gynoecium morphogenesis. *Development* **127**, 3877–3888 (2000).
39. J. J. Sohlberg *et al.*, *STY1* regulates auxin homeostasis and affects apical-basal patterning of the *Arabidopsis* gynoecium. *Plant J.* **47**, 112–123 (2006).
40. Y. Wang *et al.*, A comparison of *sun*, *ovate*, *fs8.1* and auxin application on tomato fruit shape and gene expression. *Plant Cell Physiol.* **60**, 1067–1081 (2019).
41. K. Mashiguchi *et al.*, The main auxin biosynthesis pathway in *Arabidopsis*. *Proc. Natl. Acad. Sci. U.S.A.* **108**, 18512–18517 (2011).
42. C. Won *et al.*, Conversion of tryptophan to indole-3-acetic acid by TRYPTOPHAN AMINOTRANSFERASES OF *ARABIDOPSIS* and YUCCAs in *Arabidopsis*. *Proc. Natl. Acad. Sci. U.S.A.* **108**, 18518–18523 (2011).
43. S. Yan *et al.*, Different cucumber *CsYUC* genes regulate response to abiotic stresses and flower development. *Sci. Rep.* **6**, 20760 (2016).
44. M. E. Massari, C. Murre, Helix-loop-helix proteins: Regulators of transcription in eucaryotic organisms. *Mol. Cell. Biol.* **20**, 429–440 (2000).
45. G. Toledo-Ortiz, E. Huq, P. H. Quail, The *Arabidopsis* basic/helix-loop-helix transcription factor family. *Plant Cell* **15**, 1749–1770 (2003).
46. C. Schuster *et al.*, A regulatory framework for shoot stem cell control integrating metabolic, transcriptional, and phytohormone signals. *Dev. Cell* **28**, 438–449 (2014).
47. S. Konishi *et al.*, An SNP caused loss of seed shattering during rice domestication. *Science* **312**, 1392–1396 (2006).
48. N. Arnaud, T. Lawrenson, L. Østergaard, R. Sablowski, The same regulatory point mutation changed seed-dispersal structures in evolution and domestication. *Curr. Biol.* **21**, 1215–1219 (2011).
49. Y. Dong *et al.*, Regulatory diversification of *INDEHISCENT* in the *Capsella* genus directs variation in fruit morphology. *Curr. Biol.* **29**, 1038–1046.e4 (2019).
50. D. Rodríguez-Leal, Z. H. Lemmon, J. Man, M. E. Bartlett, Z. B. Lippman, Engineering quantitative trait variation for crop improvement by genome editing. *Cell* **171**, 470–480.e8 (2017).
51. N. Panchy, M. Lehti-Shiu, S. H. Shiu, Evolution of gene duplication in plants. *Plant Physiol.* **171**, 2294–2316 (2016).
52. C. I. Ortiz-Ramírez, S. Plata-Arboleda, N. Pabón-Mora, Evolution of genes associated with gynoecium patterning and fruit development in Solanaceae. *Ann. Bot.* **121**, 1211–1230 (2018).
53. Y. Cheng, X. Dai, Y. Zhao, Auxin biosynthesis by the YUCCA flavin monooxygenases controls the formation of floral organs and vascular tissues in *Arabidopsis*. *Genes Dev.* **20**, 1790–1799 (2006).
54. J. Shen *et al.*, CsBRC1 inhibits axillary bud outgrowth by directly repressing the auxin efflux carrier *CsPIN3* in cucumber. *Proc. Natl. Acad. Sci. U.S.A.* **116**, 17105–17114 (2019).
55. T. Xin *et al.*, Genetic regulation of ethylene dosage for cucumber fruit elongation. *Plant Cell* **31**, 1063–1076 (2019).
56. Z. Zhang *et al.*, Genome-wide target mapping shows histone deacetylase complex1 regulates cell proliferation in cucumber fruit. *Plant Physiol.* **182**, 167–184 (2020).